LIGO Laboratory / LIGO Scientific Collaboration

LIGO-T1200465-v3 *Advanced LIGO* Date: 6-Aug-19

Results from Thermal Compensation System testing in the One Arm Test [public version]

Authors: Aidan Brooks

Distribution of this document:
LIGO Scientific Collaboration

This is an internal working note
of the LIGO Laboratory.

California Institute of Technology
LIGO Project – MS 18-34
1200 E. California Blvd.
Pasadena, CA 91125
Phone (626) 395-2129
Fax (626) 304-9834
E-mail: info@ligo.caltech.edu

Massachusetts Institute of Technology
LIGO Project – NW22-295
185 Albany St
Cambridge, MA 02139
Phone (617) 253-4824
Fax (617) 253-7014
E-mail: info@ligo.mit.edu

LIGO Hanford Observatory
P.O. Box 159
Richland WA 99352
Phone 509-372-8106
Fax 509-372-8137

LIGO Livingston Observatory
P.O. Box 940
Livingston, LA 70754
Phone 225-686-3100
Fax 225-686-7189

http://www.ligo.caltech.edu/

1 Introduction

The purpose of this document is to summarize the Ring Heater and Hartmann Sensor Testing undertaken as part of the One Arm Test. This document serves as a companion to the test proposal document (LIGO-T1100127: Ring Heater and Hartmann Sensor Test as part of Commissioning Advanced LIGO's First Arm cavity).

2 References

[1] Hartmann Wavefront Sensors for Advanced Gravitational Wave Interferometers, PhD Thesis, Aidan F. Brooks, LIGO Document P0900080

[2] LIGO-T1100127: Ring Heater and Hartmann Sensor Test as part of Commissioning Advanced LIGO's First Arm cavity

3 Executive Summary

3.1 Modeling:

- There is strong evidence that the existing COMSOL model for the RH underestimates the performance by ~ 29% (from HWS thermal defocus measurements described in Section 4.3.2 and cavity-scan measurements described in Section 4.4).

3.2 Ring Heater

- The ETM RH-induced curvature change is 7.9E-7 diopters per Watt.
  - The maximum electrical power that can be delivered to the RH is 40.5W.
  - The maximum curvature change is 3.2E-5 diopters per test mass.
  - The curvature change required to correct for 0.4W of absorbed interferometer power with uniform absorption is 9.0E-6 diopters.
  - Therefore, the RH has a factor of ~3.6x headroom
- **The ring heater has adequate headroom and appears to function as expected. COMSOL modeling of the RH should be improved.**

3.3 Hartmann Sensor:

- The RMS noise floor of the HWS wavefront ranged from 0.1nm at 3Hz to 1.8nm @ 1mHz for roughly 40 spots measured on the HWS
  - **Implications for ITM-HWS:** The implication for the vertex HWS (with ~900 spots) is an RMS noise floor in the wavefront ranging over [1.3nm @ 0.5Hz to 5nm @ 1mHz]. The target noise floor is ~1.4nm.
  - The low frequency noise appears white implying averaging will be possible to improve sensitivity of the ITM-HWS at the expense of measurement speed.
- The noise floor of the defocus/spherical power measured by the HWS was around $1.0 \times 10^{-5} m^{-1}/\sqrt{Hz}$ at 1mHz, referenced to the ETM, without any averaging.
  - This defocus noise floor is coherent with the measured PRISM
  - For 0.4W of absorbed power in the ETM (i.e. at full operating power) the expected defocus on a double-passed beam is 2.4E-4 m^{-1}.
  - Without any improvements to the HWS and with no averaging, the sensor can detect 30mW of absorbed power with an SNR of 2.
  - This could easily be improved with averaging (at least by a factor of 10, at most by a factor of 80 – assuming an average of 7000 images over 1000s), yielding a minimum detectable absorbed power level of 0.4 to 3mW for the ETM.
- Maximum thermal variation over 24-hr period = +/-0.06 C implies a thermally-induced error in the defocus measured by the HWS of 2.3E-8 m^{-1}.
- Interaction with ALS:
  - The HWS does not produce reliable data when the ALS laser is locked to the Arm cavity.

3.3.1 Hartmann Sensor conclusions

3.3.1.1 Secondary beam

The secondary beam is designed to monitor thermal defocus due to the ETM Transmon telescope. This is ~10^4 times smaller than the maximum expected defocus (see Section 5.3). The conclusion is that the benefit from the secondary beam is negligible vs. the extra effort and cost required to install it.

- **The secondary beam should be removed from the HWS and Transmon system.**

3.3.1.2 Permanent vs roaming installation

The HWS should be able to measure absorbed power with a precision around 1-2mW. If the IFO is initially commissioned running at 5% of maximum power then we anticipate a maximum absorbed power or ~ 20mW with 0.5ppm absorption. So this would give us a precision in measuring the absorption of around 0.05ppm from a very early stage in IFO operation. This will allow us to monitor and track the absorbed power in the ETM from a very early stage of aLIGO operation.

We can (and should) simplify the design and cost of the HWS by removing the secondary beam and temperature sensors. However, the effort required to align and install the optics necessary to image the ETM on the HWS (the optical layout is detailed in D1100607) was considerable. Removing and replacing these optics every time a measurement is required would hamper a system designed for quick testing. Even though we might not use it all the time, we will be well served by having a permanent HWS installation at each ETM.

- **We recommend a permanent HWS installation at each ETM**

4 Detailed Summary

4.1 Ring Heater Electrical function:

After some initial calibration issues, both ITM and ETM ring heaters were confirmed to be functioning as required[1].

The RH I/O interface functioned without issues. The calibration of all four RH segments is documented in Section 7.1. The resistance of all four RH segments was within 1.3 Ohms of the target resistance of 36 Ohms.

4.1.1 Tasks not completed

- The BSC temperature was not recorded.
- No testing of ground loops was performed.
- The maximum current of the RH drivers was not investigated thoroughly.
- The RH temperature sensor was not tested.

4.2 Ring Heater-Suspension (SUS) interaction

The RH-SUS interaction was not investigated due to time constraints.

4.3 Ring Heater Thermal profile

4.3.1 Characterize the ITM/ETM RH-induced tilts

The ITM/ETM RH-induced tilts were not investigated due to time constraints.

4.3.2 Ring heater long-term measurements

The RH was turned on to dissipate 6.3W of electrical power. The RH thermal lens was measured with the Hartmann sensor over a 12-hour period. This system was also modeled in COMSOL – illustrated in Figure 1.

[1] The Ring Heater Drivers are to be replaced with newer versions after the OAT. These will interface to the EtherCAT controls system, rather than the Real Time System.

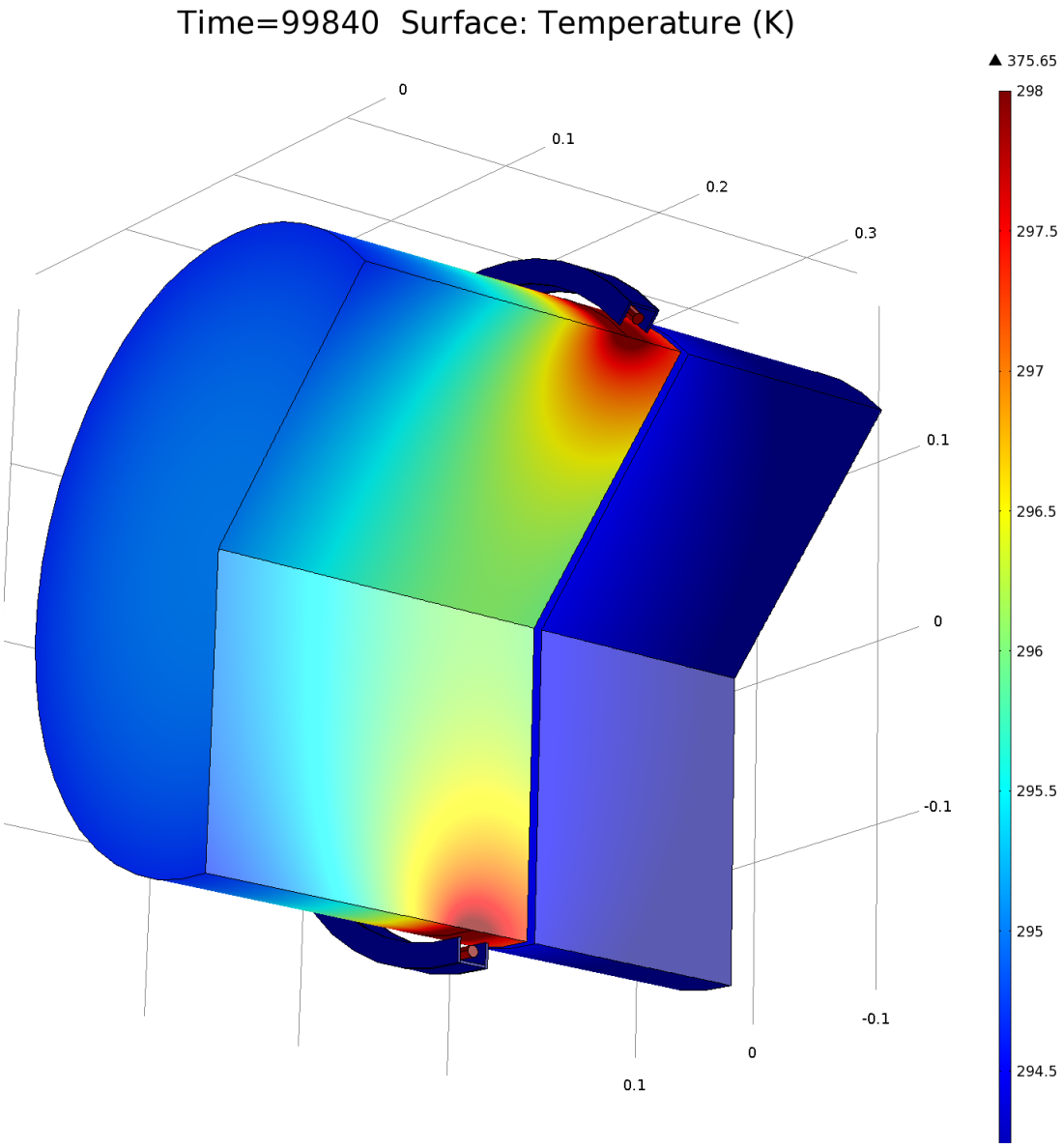

Figure 1: A 2D axi-symmetric model of the ETM, CP and shielded RH. The ETM, CP and RH are all radiatively coupled.

The temporal evolution of the thermal lens, characterized by the defocus, qualitatively followed what was predicted by a COMSOL model of the ETM+CP pair, however there were distinct quantitative differences as illustrated in Figure 2. The HWS thermal lens is ~29% larger than the predicted thermal lens by COMSOL at t = 10 hours. Additionally, COMSOL predicts that the thermal lens should form faster than what we see (by ~1000s) and predicts a higher maximum to steady-state ratio than what we see.

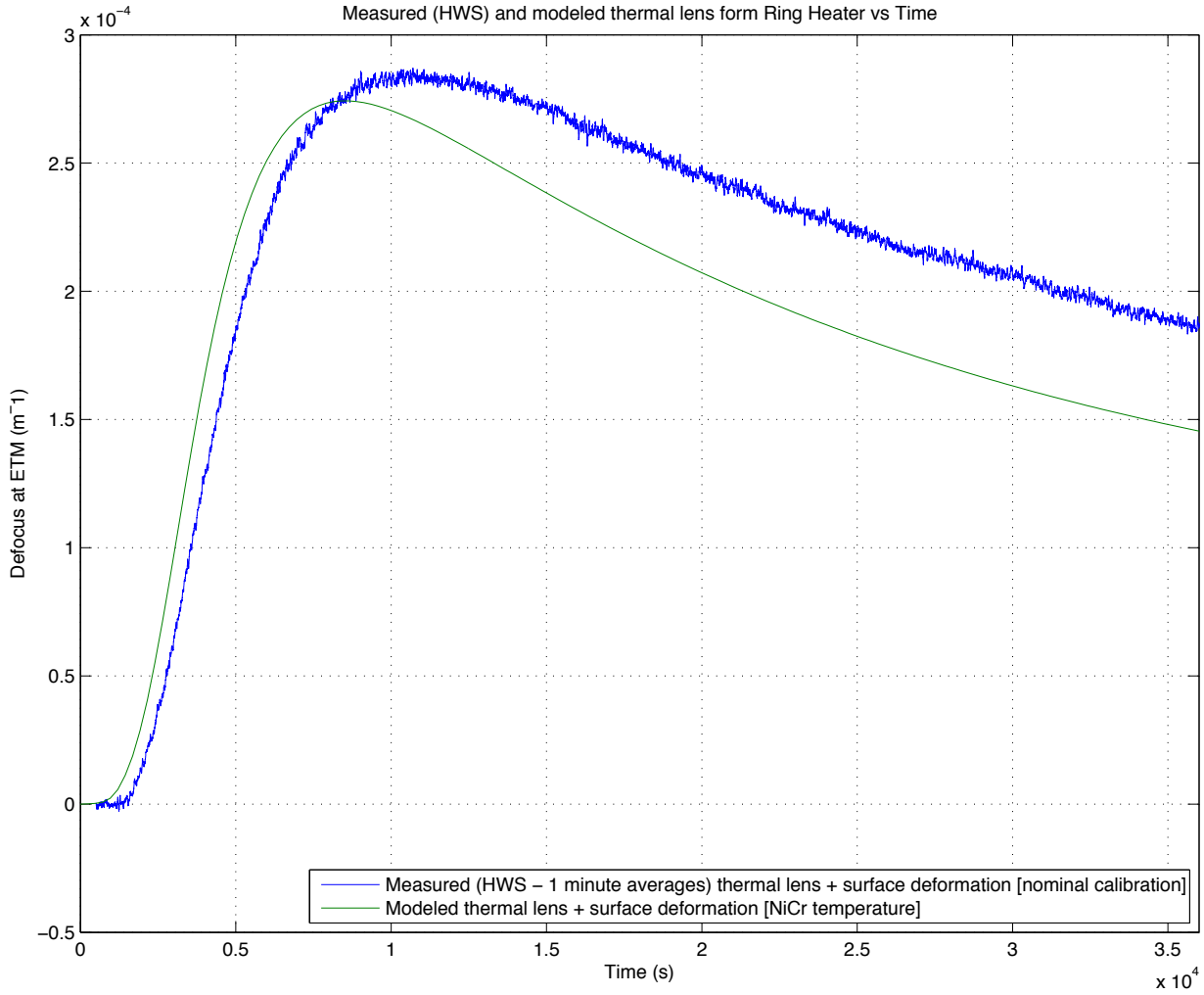

Figure 2: ETM+CP RH-induced thermal lens measured by HWS (blue) and predicted by COMSOL (green)

4.4 Ring Heater Cavity G-factor measurements

The 4-km FP arm was scanned to measure the frequency response of the cavity. Several higher order spatial modes were located in this cavity scan, as illustrated in Figure 3. The frequency of these modes was measured to measure the cavity g-factor (and the ETM HR surface RoC). The experimental method and injection scheme is explained in detail in the following LHO alog entry: Cavity scan methodology, https://alog.ligo-wa.caltech.edu/aLOG/index.php?callRep=4033.

The ETM RH was applied at 13.3W to measure the change in the higher order mode spacing as a function of time. The results were compared to the COMSOL model described in the previous section and are illustrated in Figure 4. These results show that the measured change in the RoC is approximately 29% larger than the predicted change in the RoC.

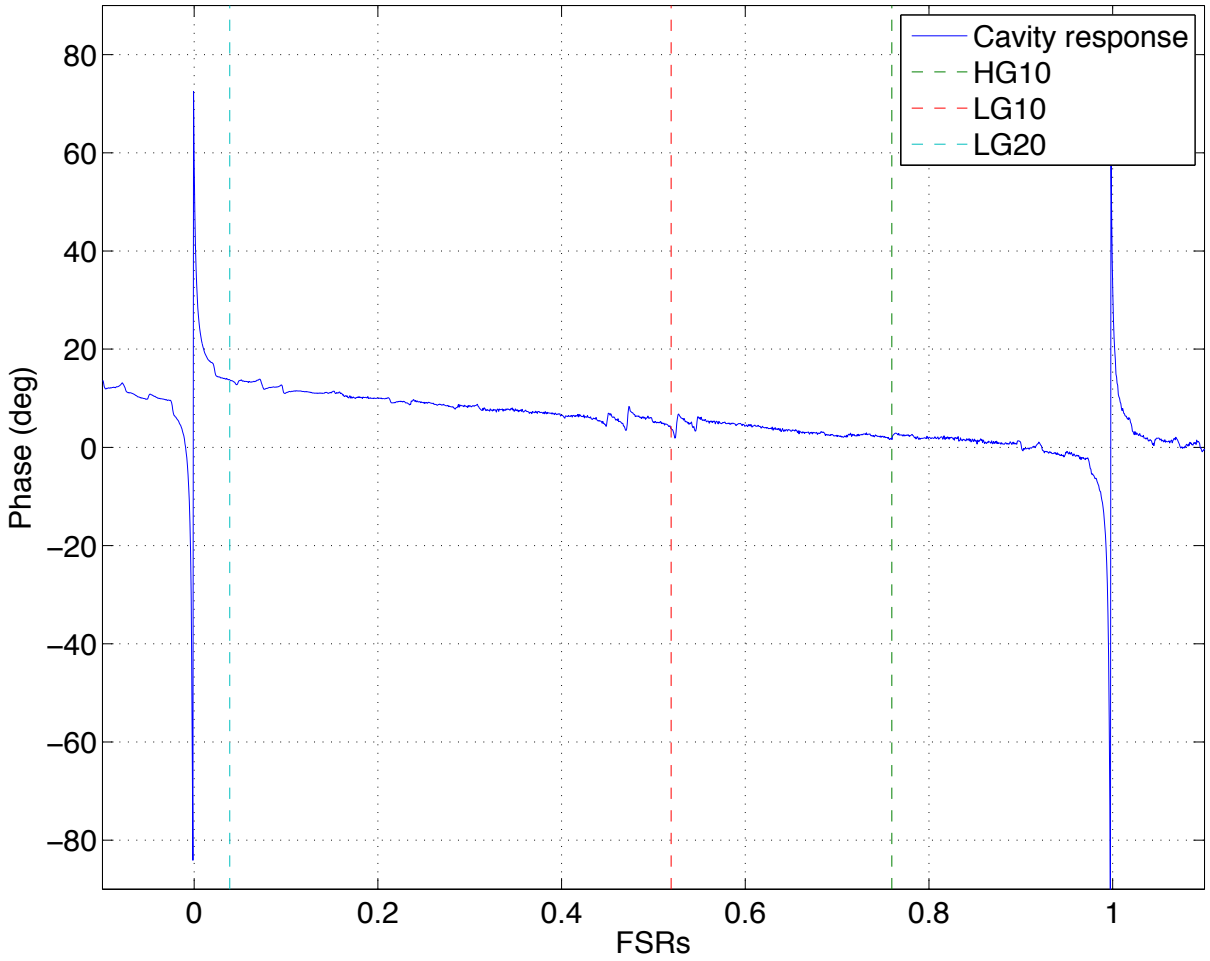

Figure 3: The phase response from a single cavity scan of the 4-km FP arm cavity. The HG10, LG10 and LG20 higher order modes are highlighted.

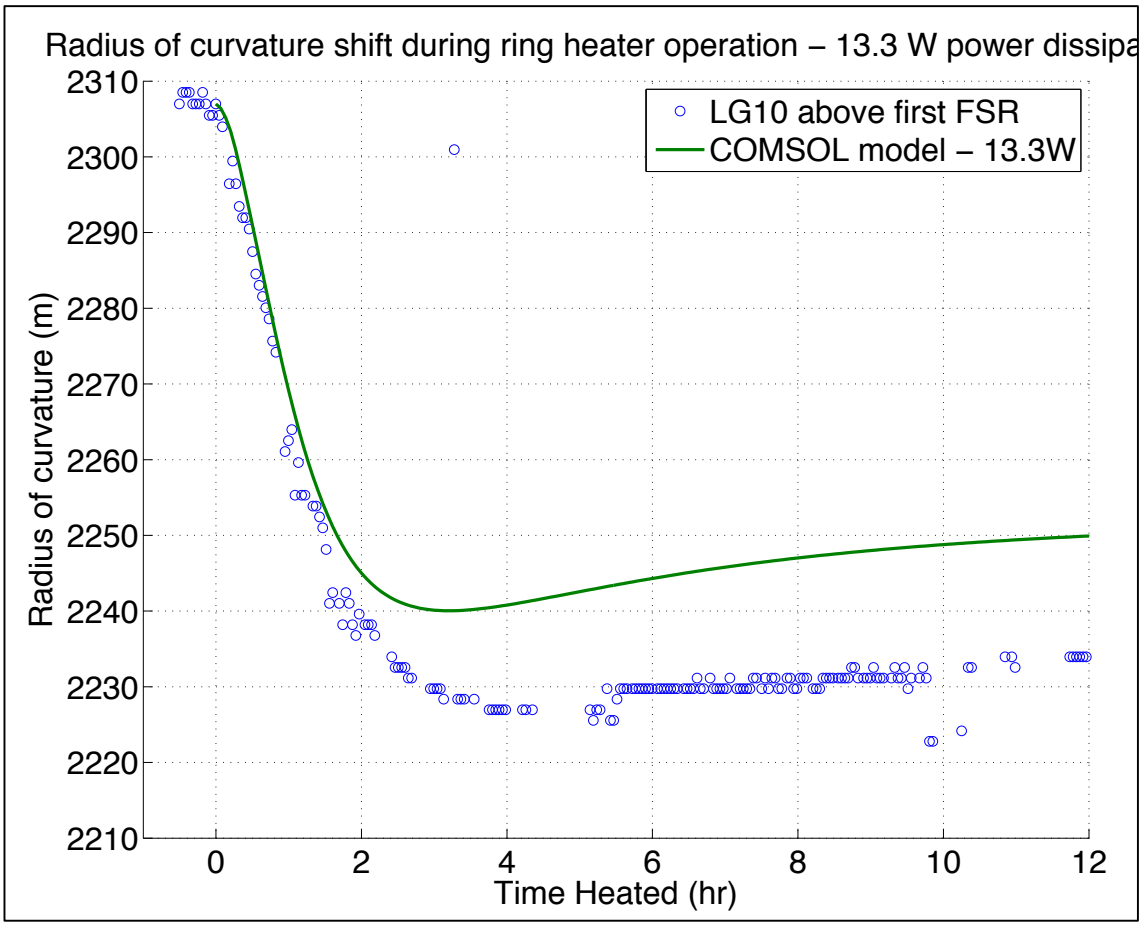

Figure 4: Measured radius of curvature change in ETM (inferred from LG10 frequency shift) and results predicted by COMSOL model [TCS_SVN/aLIGO/test data/OneArmTest/h2hwsey/2012_09_14_ETM_rh_cavity_scan_13W]

4.5 Ring Heater performance summary

The Ring Heater induced a change in the RoC of ~ 4.2 m/W, or an optical power change of 7.9E-7 m^{-1}/W. The RH drivers deliver a maximum current of 750mA per segment, or 20.25W per segment. This yields a maximum optical power change of 3.2E-5 m^{-1}/W for 40.5W of electrical power delivered to the ETM.

5 Hartmann sensor (HWS) testing

5.1 HWS basic function

5.1.1 CDS Interfaces

- All desired EPICS HWS channels were successfully recorded to frames.

Issues:

- HWS computer occasionally failed or report problems with the disk (approximately 3 or 4 times over the 3 month OAT period).
- All code was stored locally on the HWS computer and not in the `target` directory on the h2boot machine.

5.1.2 Imaging of the ETM HR surface

- Imaging of the ETM HR surface was accomplished by injecting a sinusoidal signal into the yaw of the ETM and measuring the position of the beam on the HWS CCD.
    - We did not use the method proposed in T1100127 – simultaneously measuring the yaw and position with the Hartmann plate in place.
    - Instead, we removed the Hartmann plate and measured the centroid of the Gaussian spot on the CCD.
    - The image plane of the ETM was located by translating the first lens in the imaging telescope along the optical axis until the amplitude of the oscillation on the CCD was minimized, as illustrated in Figure 5.
    - The Hartmann sensor was then moved 11 mm (the distance between the CCD and the Hartmann plate) further along the optical axis to place the image plane of the ETM on the Hartmann plate.

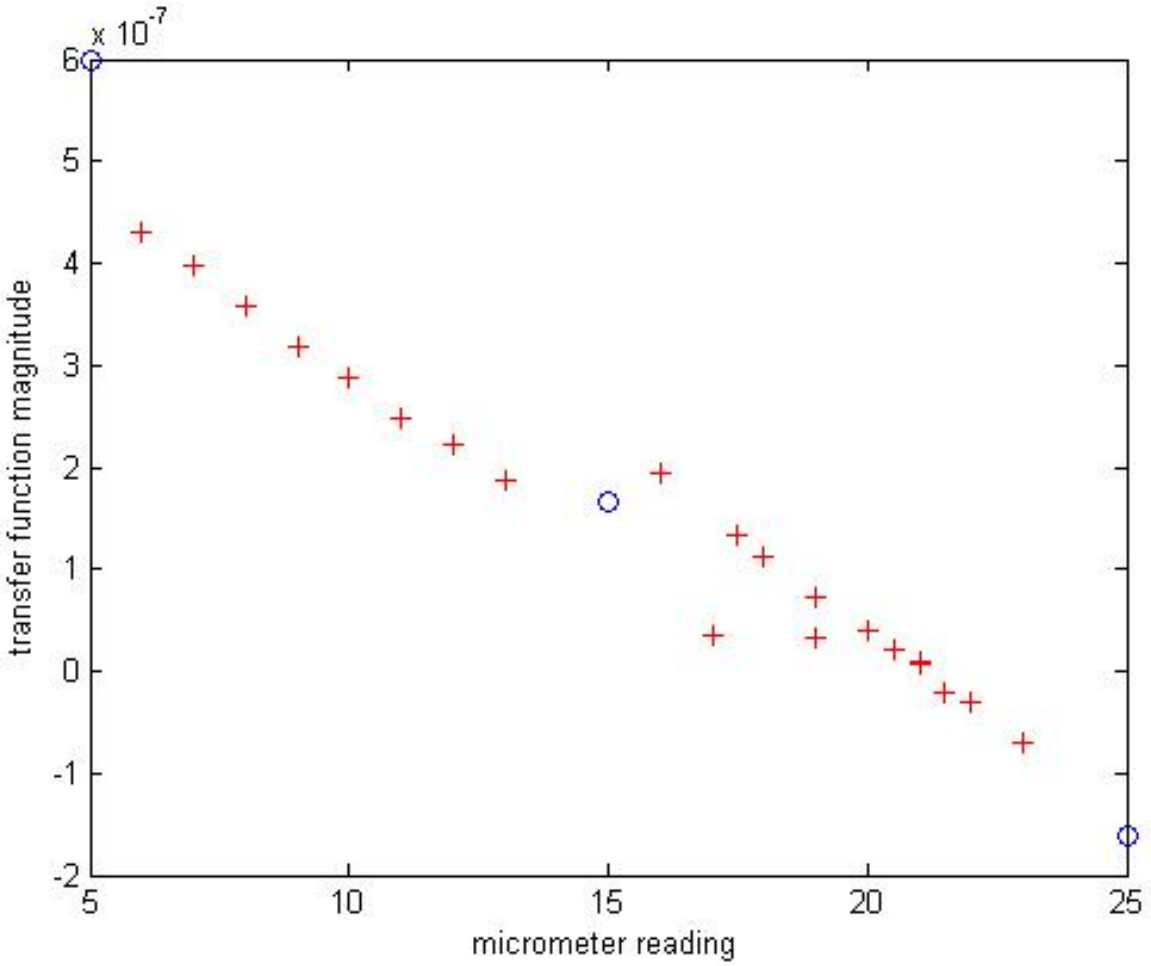

Figure 5: CCD oscillation amplitude/injected amplitude ratio vs imaging Lens micrometer reading. https://alog.ligo-wa.caltech.edu/aLOG/uploads/3404_20120711133108_transferfunction11july.jpg

Issues:

- The noise in the originally proposed pitch measurement is concerning. This could potentially indicate some issue with interference fringes on the Gaussian spot.

5.1.3 HWS probe and secondary beam shape

The secondary beam was not used.

The probe beam shape showed evidence of interference fringes. Some of these were due to the polarizing beam splitter (PBS) in the optical layout and disappeared when this was replaced with a mirror. There were some residual fringes that remained with an unidentified source, as shown in Figure 6. The best guess for these was the viewport.

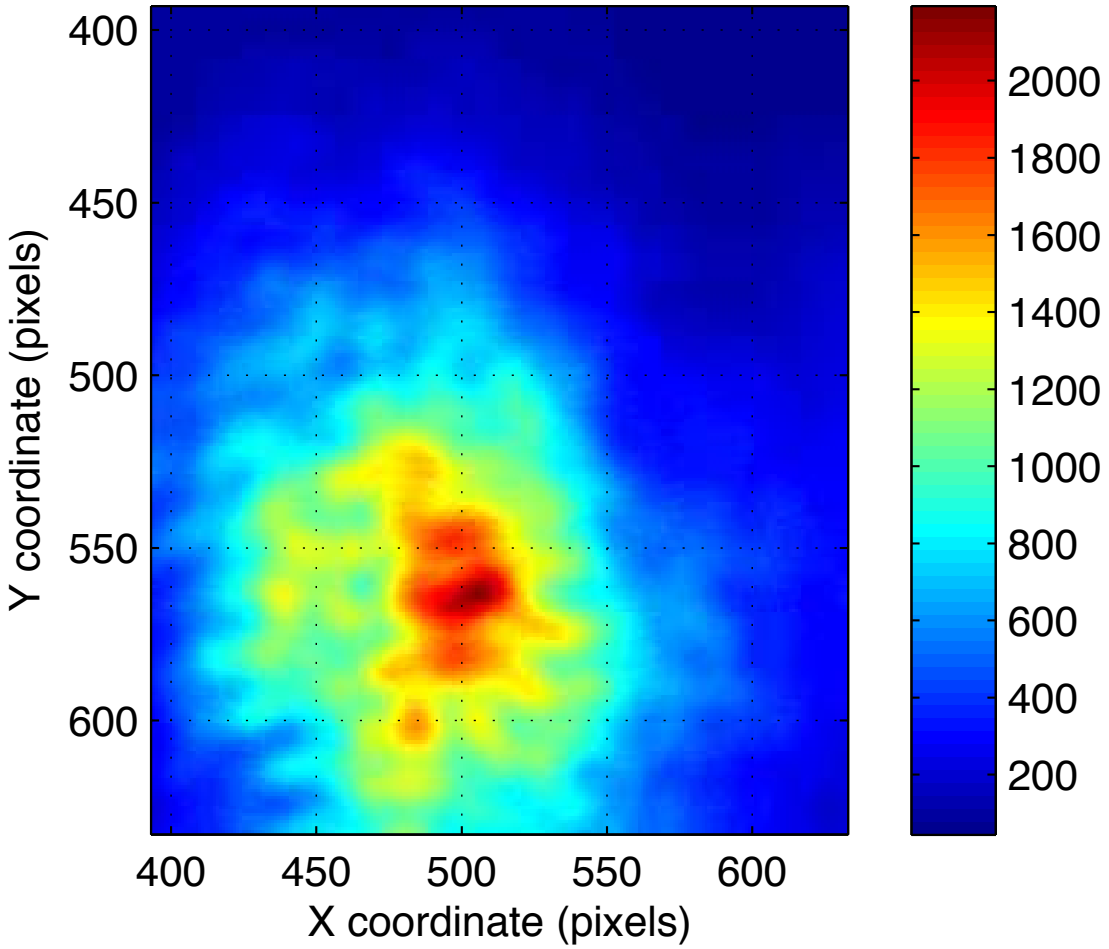

Figure 6: Beam profile on HWS CCD

5.1.4 Calibration of HWS signal

The HWS signal was not calibrated using the optical lever. Instead, precise and accurate measurements were made of the imaging optic locations to determine the magnification between the ETM and HWS.

Additionally, the HWS lever arm was calibrated in-situ using an interferometric measurement of the angle between two different beams and the measured displacement of Hartmann spots from the same two beams.

5.2 Quiescent HWS tests

5.2.1 Quiescent noise floor

Definitions:

- $\sigma_{\Delta W}$, standard deviation in the wavefront between two neighbouring spots. It is equal to the product of the standard deviation of all the gradient measurements across the Hartmann sensor multiplied by the distance between neighbouring spots.

- σ_W, standard deviation in the reconstructed wavefront

Using the analysis detailed in Section 3.3.5.3 of [1], the RMS wavefront error, σ_W, is:

$$\sigma_W = \sqrt{C_S}\sigma_{\nabla W} ,$$

where C_S is the Southwell noise coefficient shown in Figure 3.20 in [1] and reproduced below in Figure 7.

The ETM-HWS was run in a quiescent state for a 7-hour period and the amplitude spectral density of the RMS wavefront error was determined (after removing PRISM). This is shown in Figure 8. The RMS error of the wavefront ranged from 0.1nm at 3Hz to 1.8nm @ 1mHz for the roughly 40 spots used in the ETM HWS.

This measurement can be extrapolated to the ITM-HWS by recalculating σ_W for 700 spots instead of 40. The implication for the ITM HWS (with ~700 spots) is an RMS wavefront error ranging over [1.3nm @ 0.5Hz to 5nm @ 1mHz]. Overall, the noise floor will be ~ 2.7x higher than the ETM HWS. This is also shown in Figure 8.

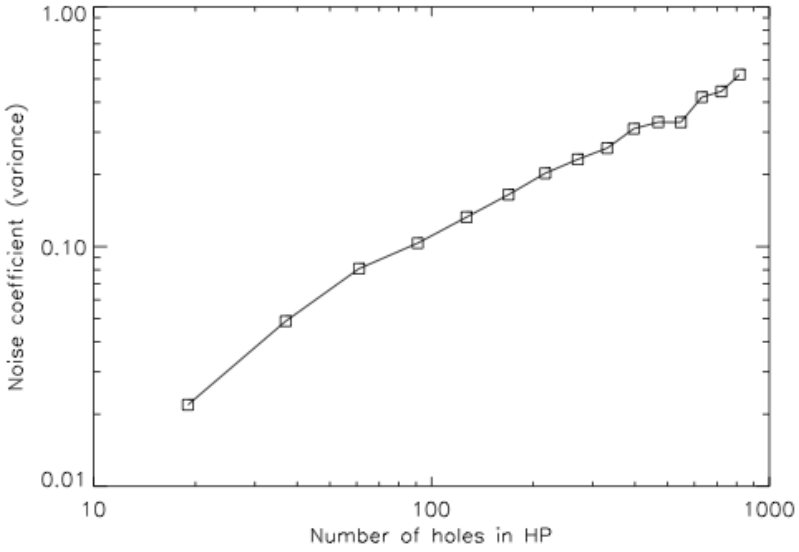

Figure 7: The Southwell noise coefficient, C_S, of the Gauss-Seidel iterative matrix wavefront reconstruction versus the number of holes in the Hartmann Plate.

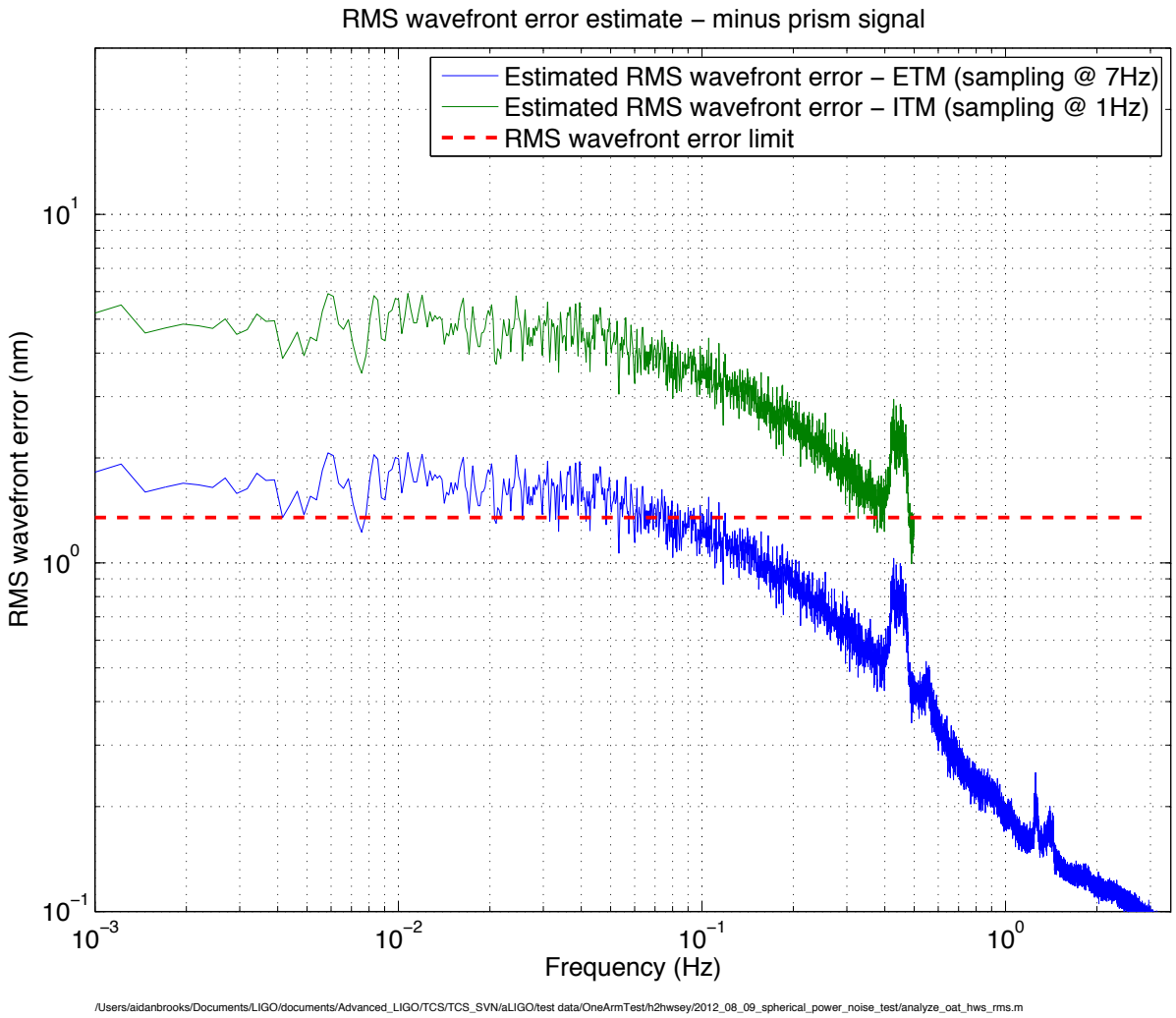

Figure 8: Amplitude spectral density of the RMS wavefront error for the ETM and, estimated, for the ITM.

It appears that the HWS is limited by an undetermined white noise source at low frequencies (below 50mHz). It is expected, then, that we can improve the noise floor of the HWS by averaging many results at the expense of measurement speed.

- ETM HWS: averaging two measurements should reduce the RMS noise floor <= 1.35nm for all frequencies above 1mHz. Max. operating frequency = 3.5Hz.
- ITM HWS (predicted): averaging ~14 measurements should reduce the RMS noise floor to 1.35nm. Max. operating frequency = 70mHz (1 measurement every 14s).

5.2.2 Quiescent defocus (P and S beams)

The defocus of the secondary beam was not measured.

The defocus noise floor of the probe beam was measured and the results are plotted in Figure 9.

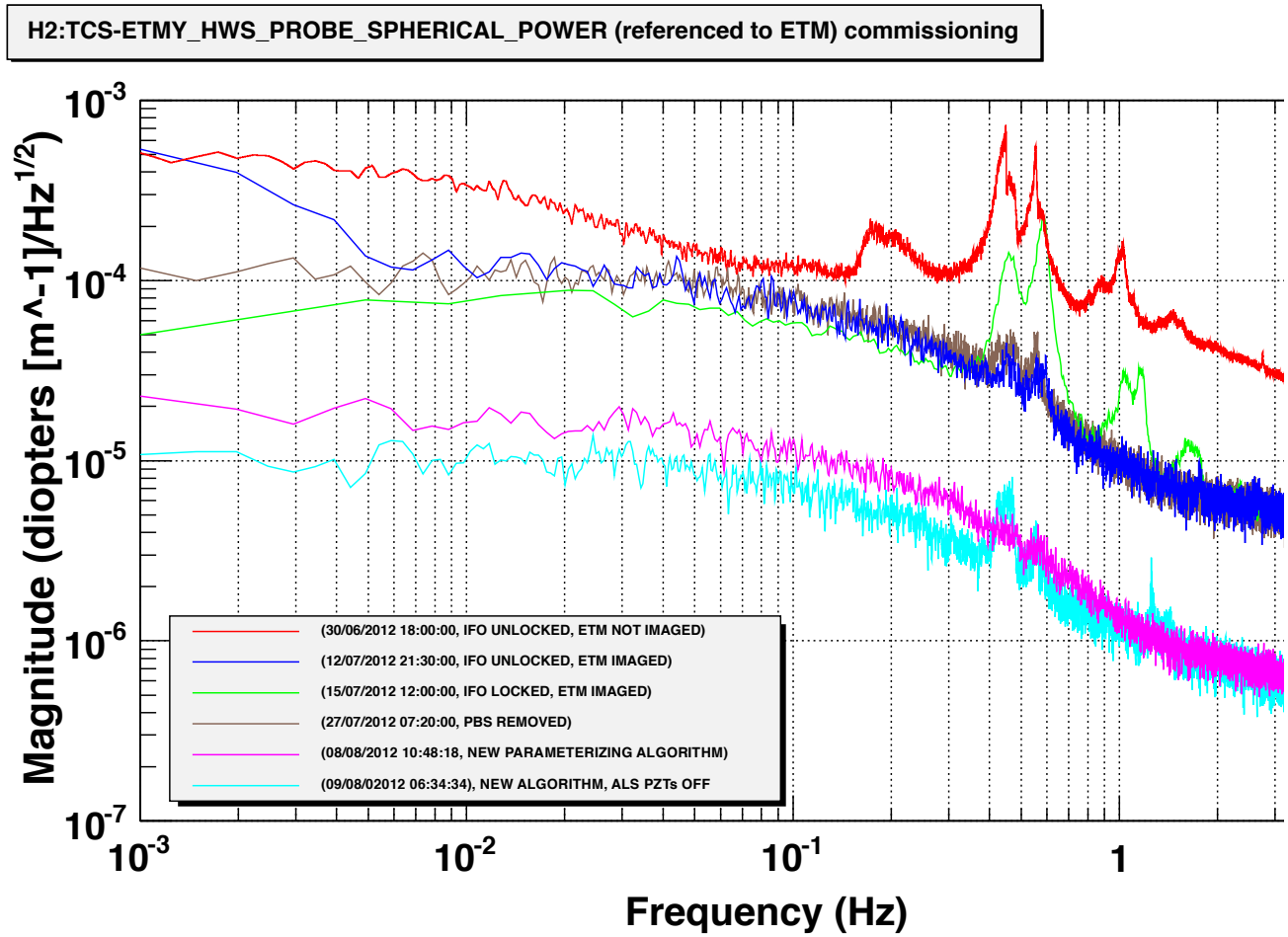

Figure 9: HWS probe beam defocus noise spectra over the duration of the OAT. The shot-noise floor is approximately 6E-7m^{-1}/rtHz.

The most significant improvements in the noise floor of the measured defocus (from 1E-4 m^{-1}/rtHz to from 1E-5 m^{-1}/rtHz at 1mHz) were made when we reduced the number of optical aberrations that we fitted to from 8 to 4 (from up to 4th order to only up to 2nd order). These factor of 10 improvement at 1mHz is a factor of 7x larger than we expect: (reducing the number of fitting parameters by a factor of 2 should reduce the noise in those parameters by a factor of SQRT[2]). The University of Adelaide is studying these results closely.

There is strong coherence between the SPHERICAL_POWER and PRISM_X/Y measured by the HWS below ~100mHz.

The temperature variation of the HWS plate is shown in Figure 10. The temperature varied, on average, by +/- 0.06C over a 24-hour period. The thermally induced defocus coefficient for the HWS is approximately 1.5E-4 m^{-1}/K at the HWS, or 3.8E-7 m^{-1}/K referenced to the ETM. Therefore, the thermally induced defocus at the ETM should vary by +/- 2.3E-8 m^{-1} over a 24-hour period. This is nearly 3 orders of magnitude lower than the measured noise floor.

The HWS and table temperature sensors are not necessary.

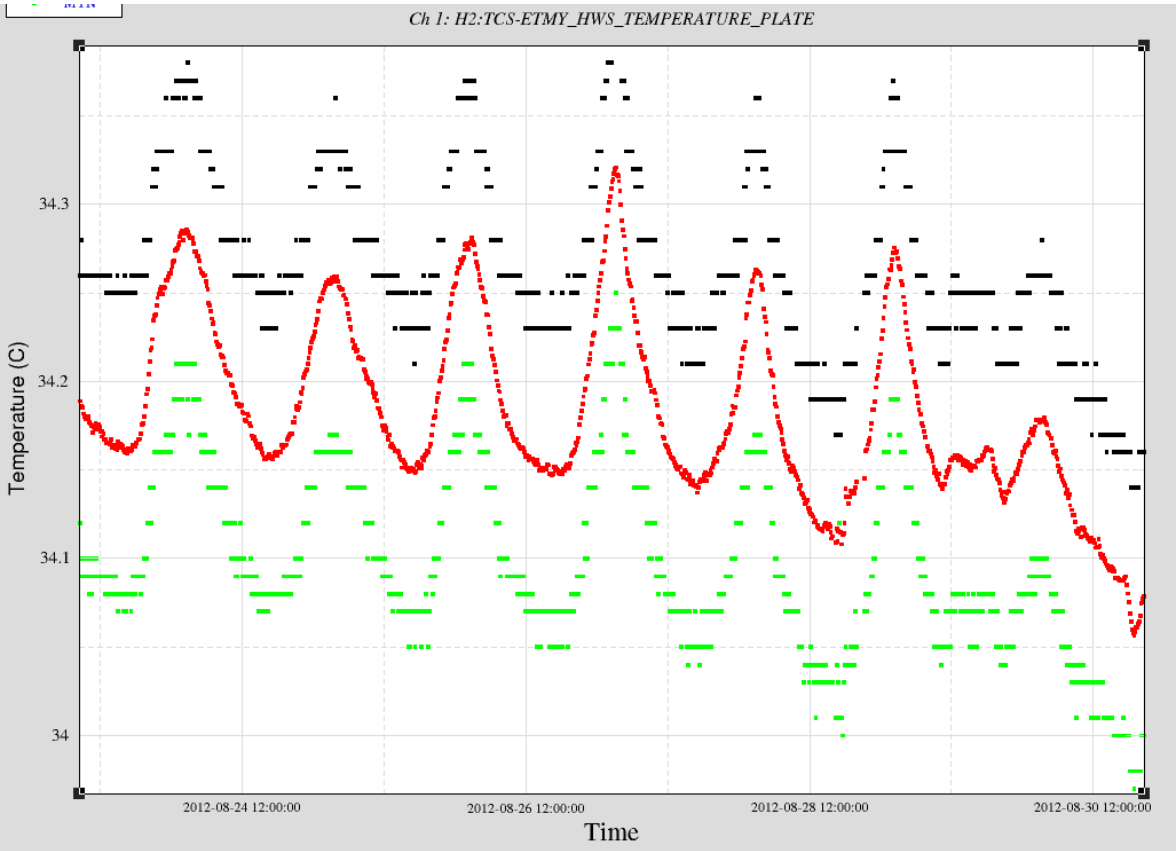

Figure 10: Temperature (in deg C) of ETM Hartmann plate over an 8-day period.

The prism spectra were not investigated.

5.3 Hartmann sensor conclusions

The purpose of the Hartmann sensor at the ETM is envisioned as diagnostic primarily to monitor the absorbed power in the ETM. A secondary effect is to monitor the performance of the ETM ring heater. The primary purpose would be achieved by monitoring changes in the ETM thermal lens as the interferometer power was increased or decreased. This would be accomplished by resetting the HWS reference or baseline measurement before the IFO power was varied and then measuring the change in the thermal lens. This procedure would take between 1 and 3 hours.

- We determined from the OAT that measured temperature change in the Hartmann sensor (and presumably the in-vacuum telescope), is small over this time scale: of the order of 15mK.
- The resulting thermal defocus is of the order of 6E-9 m^-1 from the HWS and 1.7E-8 m^-1 for the Transmon telescope.
- This brings the total thermal defocus for the ETM HWS to around 2.3E-8 m^-1.
- The expected defocus in the ETM for the nominal 0.4W of absorbed power at full power is 2.3E-4 m^-1.
- The total thermal defocus is approximately 10^4x smaller than the maximum expected signal.

6 Interaction with ALS

The Hartmann sensor measurements of the thermal lensing were performed when the cavity was misaligned. The intensity distribution and power on the probe beam fluctuate significantly when the ALS was in operation, rendering the HWS inoperable.

7 Results

7.1 RH calibration

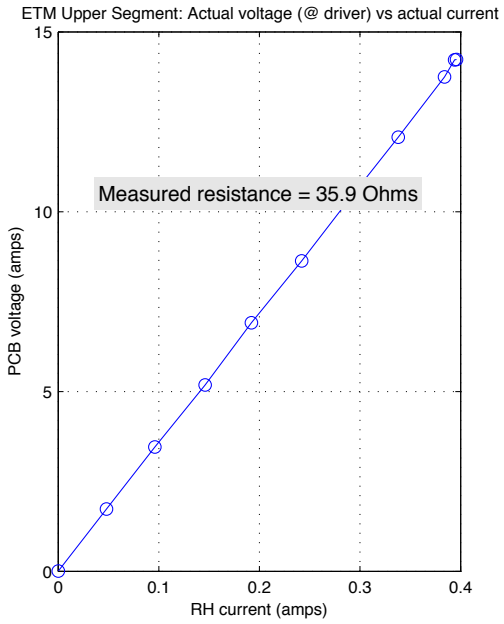

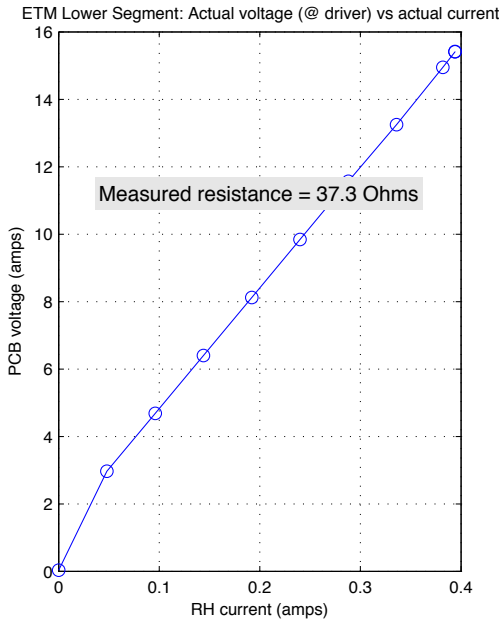

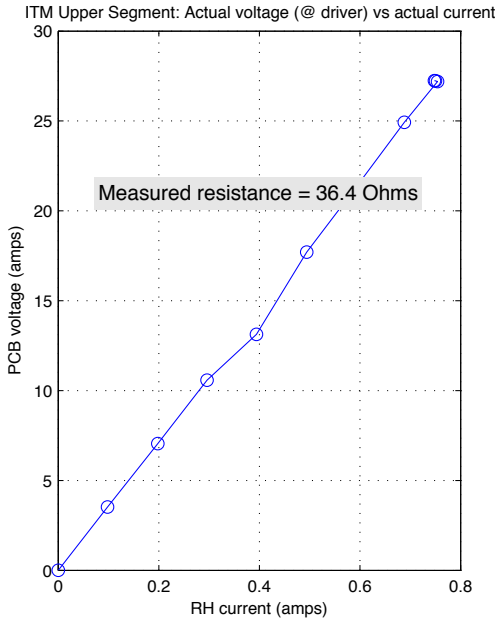

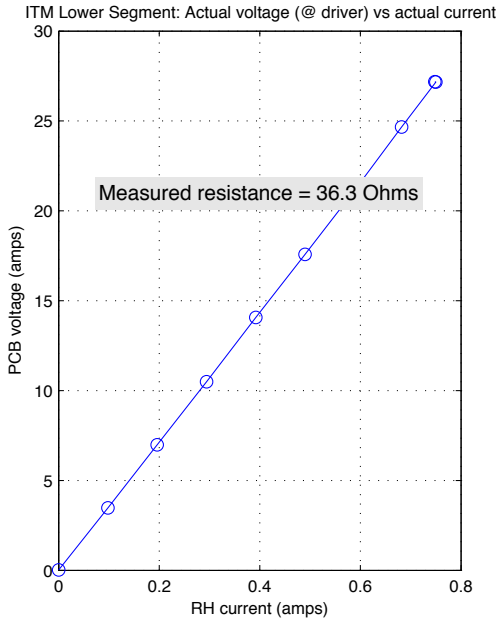

/Users/aidanbrooks/Documents/LIGO/documents/Advanced_LIGO/TCS/TCS_SVN/aLIGO/test data/OneArmTest/h2hwsey/2012_09_09_rh_calibration/ETM_ITM_RH_calibration.m

8 Glossary

- PRISM: the coefficient of the linear component a wavefront, for example, the terms P_x and P_y in the following equation:

$$W(x,y) = P_x x + P_y y + \ldots$$

- SPHERICAL POWER (sometimes called *defocus*): the coefficient of the r^2 component of a wavefront, e.g. the term S in the following equation:

$$W(x,y) = \frac{S}{2}\left(x^2 + y^2\right) + \ldots$$